This article has been accepted for publication in a future issue of this journal, but has not been fully edited. Content may change prior to final publication. Citation information: DOI 10.1109/ACCESS.2020.3029068, IEEE Access

Digital Object Identifier

Fractional-order Predictive PI Controller for Dead-Time Processes with Set-point and Noise Filtering

P. ARUN MOZHI DEVAN[1] **(Graduate Student Member, IEEE), FAWNIZU AZMADI HUSSIN**[1] **(Senior Member, IEEE) and ROSDIAZLI IBRAHIM**[1] **(Senior Member, IEEE), KISHORE BINGI**[2] **(Member, IEEE), HAKIM ABDULRAB**[1] **(Graduate Student Member, IEEE)**

[1]Department of Electrical and Electronics Engineering, Universiti Teknologi PETRONAS, Seri Iskandar 32610, Malaysia
[2]Department of Control & Automation, School of Electrical Engineering, VIT University, 632014 Vellore, India

Corresponding author: Arun Mozhi Devan Panneer Selvam (arundevaeie@gmail.com)

This work was supported by Universiti Teknologi PETRONAS through Yayasan UTP Fundamental Research under the Grant Y-UTP 015LC0-045.

ABSTRACT

In most of the industrial process plants, PI/PID controllers have been widely used because of its simple design, easy tuning, and operational advantages. However, the performance of these controllers degrades for the processes with long dead-time and variation in set-point. Up next, a PPI controller is designed based on the Smith predictor to handle dead-time processes by compensation technique, but it failed to achieve adequate performance in the presence of external noise, large disturbances, and higher-order systems. Furthermore, the model-based controllers structure is complex in nature and requires the exact model of the process with more tunable parameters. Therefore, in this research, a fractional-order predictive PI controller has been proposed for dead-time processes with added filtering abilities. The controller uses the dead-time compensation characteristics of the Smith predictor and the fractional-order controller's robustness nature. For the high peak overshoot, external noise, and disturbance problems, a new set-point and noise filtering technique is proposed, and later it is compared with different conventional methods. In servo and regulatory operations, the proposed controller and filtering techniques produced optimal performance. Multiple real-time industrial process models are simulated with long dead-time to evaluate the proposed technique's flexibility, set-point tracking, disturbance rejection, signal smoothing, and dead-time compensation capabilities.

INDEX TERMS Dead-time compensation; filtering; fractional order controller; PID control; process control.

I. INTRODUCTION

Simple control structure and easy tuning parameters made the PID controller trustworthy in process industries even after the emergence of new process control strategies like model-based controllers, adaptive control, fault tolerance control, etc., [1]–[3]. PI controller is largely adopted in the process and automation industry among all the PID variants [4], [5]. Even though the derivative action in a PID controller leads to phase advance due to its predictive capability, it becomes problematic when long dead-time and high-frequency noise are involved because of the noise sensitivity introduced by the derivative part [6], [7]. Therefore, conventional PI controllers are inadequate to be employed in a delayed environment, high-frequency noise, and other uncertainty systems [8]–[10]. In such environments, if the PI controllers are used, the system will lead to oscillatory and unstable response because of the limited gain constant [11], [12]. For instance, if the gain is small, the response of the system becomes sluggish. On the other hand, if the gain is large, the response becomes oscillatory with high peak overshoot and may lead to system instability. Several enhancements in conventional PI controller resulted in the development of different controllers like fractional-order PI (FOPI), set-point weighted PI (SWPI), predictive PI (PPI), and nonlinear PI (NPI) which are utilized by various researchers to control processes with long dead-time [13]–[16].

This article has been accepted for publication in a future issue of this journal, but has not been fully edited. Content may change prior to final publication. Citation information: DOI 10.1109/ACCESS.2020.3029068, IEEE Access

On the other hand, hybridizing the PI controller with the advanced control techniques like dead-time compensators (DTC), model-based predictive controller (MPC), internal model controller (IMC), and generalized predictive controller (GPC) to enhance its performance were carried out by various researchers [17]–[19]. Even though all the above approaches improved the controller performance, they failed to withstand in the industrial processes because of their complex design, more added tuning parameters, maintenance, and implementation difficulty. Many of these controllers need an exact process model to achieve an optimized control [17], [18]. To highlight the above discussed constraints and drawbacks, the various controllers and process model parameters needed to be tuned are shown in Table 1.

TABLE 1. Tunable parameters of various controllers

Controller	Model Parameter			Controller Parameter		
PI	-	-	-	Kc	Ti	-
FOPI	-	-	-	Kc	Ti	λ
PPI	-	-	Lp	Kc	Ti	-
FOPPI	-	-	Lp	Kc	Ti	λ
Smith predictor	K	T	Lp	Kc	Ti	-
IMC	K	T	Lp	-	Tcl	-

Control of dead-time processes is comprehensively researched because most of the real-time industrial process exhibits the inherent time delay. In these situations, increased phase lag in PI controllers will lead to the destabilization of the closed-loop control system. Researchers in [6], [20]–[22] came up with a new predictive PI controller which is based on conventional PI and Smith predictor to solve these issues faced by the process plants with longer dead-time. However, the controller is unable to achieve robust performance during large disturbances and shows poor closed-loop performance due to the mismatch between the real-time plant and the designed process model. Conventional PI controller is also a type of fractional-order control that will be obtained by making the fractional-order parameter lambda (λ) value equal to unity (i.e. λ=1) in the integral part of the PI controller. I. Podulumby [23] first proposed these modifications in the conventional controller. This adjustable parameter gives a way for achieving the most flexible and dynamic properties of the fractional controller [24]–[26]. As a result, the fractional-order controllers are extensively used in many engineering control applications like process industries, unmanned aerial vehicles (UAV's), military applications, trajectory tracking etc., [27]–[33]. Among these applications, some of the researchers designed the fractional-order controllers for dead-time process plants [34]–[36]. Results have shown that the fractional-order PI controller produced robust control actions but settled slower and produced higher overshoot than the conventional methods. Also, an extensive review of the recent advances in fractional-order control for the time delay process can be found in [37]. Therefore still, there is a need for designing an adequate controller to achieve robust performance even in the presence of longer dead-time.

Earlier literature is discussed about the presence of external noise, set-point variation and longer dead-time in the real-time process makes it more difficult to control. Thus, alternate approaches like set-point filtering are introduced for preventing the large variation in the control signal often results in high peak overshoot which fastens the wear and tear of components in final control elements. Vijayan et al. [38] proposed this filtering to solve this issue. But this method involves tedious calculations and the user has to define multiple parameters to obtain the filter time constant. Also, this method did not reduce much overshoot in closed-loop processes. For example, their filter time constant calculation will be given as:

$$T_f = \tau\left(\frac{k - Mp2 - k * e^{-tp2/\tau}}{k - Mp2}\right)$$

where, τ - filter time constant; k- system gain ($k = \frac{Mp1}{0.6321}$); tp - peak time; Mp - peak overshoot.

At the same time, processes associated with noise often experience the control signal fluctuations due to the regulatory performance degradation [39]–[41]. Therefore, filtering is needed to remove the noise signal from the process signal to get the effective control signal output. In [17], [42], [43] researchers proposed various filtering techniques to deal with the external noise and set-point variation problems. These results indicated that it is not essentially higher order filters that are needed to achieve good performance in the PI controller. Thus a new first-order filter is designed without changing the conventional structure and it is compared with the existing techniques.

The issues observed in the above literature motivated and led to the intention of developing a new control technique that improves the dead-time process performance. On the other hand, the external disturbance and noise presence in most of the process control applications led to the idea of developing a filtering technique based on existing and extensively adopted techniques. The major contributions to the field of process control from this research paper will be given as follows:

1) A new fractional-order predictive PI (FOPPI) controller is designed by hybridizing the traditional fractional-order PI and the predictive PI (PPI) controller.
2) A new first-order filter is designed by including the process model parameters such as process gain (K) and dead-time (L_n) in the filter time constant (T_f).
3) Proposed controller performances are compared against the PI, PPI, and FOPI controllers. While the proposed filter performances are compared with the widely adopted Hagglund [42] and Normey [17] filter.

The remaining sections of the paper are organized as follows: A detailed design procedures for the proposed fractional-order predictive PI (FOPPI) controller and new filtering techniques are presented in Section II. Section III provides the simulation results and analysis of the various real-

This article has been accepted for publication in a future issue of this journal, but has not been fully edited. Content may change prior to final publication. Citation information: DOI 10.1109/ACCESS.2020.3029068, IEEE Access

time processes plants. Filter simulation results are illustrated in Section IV and V. Conclusion and future developments of the proposed work are given in Section VI.

II. METHODOLOGY

Design of the proposed FOPPI controller using the conventional fractional-order PI controller and the smith predictor is elucidated in the first part. Later, major signals like the input signal R(s) and process feedback signal Y(s) are fed to the set-point filter and noise filter respectively to improve the process stability. A new approach for set-point and noise filtering technique is introduced and it is compared with other filter designs from Hagglund [42] and Normey [17] to evaluate its performance and efficacy.

A. FRACTIONAL-ORDER PI (FOPI) CONTROLLER

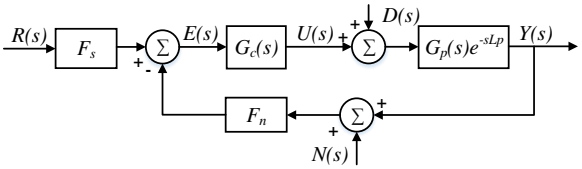

FIGURE 1. General block diagram of a closed-loop control system with set-point and noise filter.

Consider the traditional closed-loop feedback control system of Fig. 1, $G_c(s)$ is the controller, $G_p(s)$ is the process plant, $N(s)$ and $D(s)$ represents the external noise and disturbance, and control signal and error signal are represented as $U(s)$ and $E(s)$. All the system signals and process variables are represented in Laplace domain. Consider $G_c(s)$ is the PI controller in the Fig. 1, the control signal of PI controller is given as:

$$U(s) = K_p\left(1 + \frac{1}{T_i s}\right)E(s) \tag{1}$$

where, K_p and T_i are the proportional gain and integral time constants of the controller. Fractionalize the integral action using λ of the above PI controller equation (1) yields the fractional-order PI (FOPI) controller. Hence, the fractional-order PI controller control signal will be represented as:

$$U(s) = K_p\left(1 + \frac{1}{T_i s^\lambda}\right)E(s),\ 0 < \lambda < 1 \tag{2}$$

In Eqs. (1) and (2), the error signal $E(s)$ is given as,

$$E(s) = R(s) - (Y(s) + N(s)) \tag{3}$$

Oustaloup's approximation technique is used in fractional-order integrator $1/s^\lambda$ considered in Eq. (2).

B. FRACTIONAL-ORDER PREDICTIVE PI (FOPPI) CONTROLLER

Consider the First-Order Plus Dead-Time (FOPDT) process with fractional integrator as:

$$G_p(s) = \frac{K}{1 + Ts^\lambda}e^{-sL_p} \tag{4}$$

In the above equation, K, L_p, T, and λ are the process gain, dead-time, time constant, and fractional order integrator, respectively. Using the block diagram in Fig. 1, if $G_c(s)$ is the fractional-order predictive PI controller, the control signal $U(s)$ will be obtained by considering the First-Order Plus Dead-Time (FOPDT) transfer function of $G_p(s)$.

Closed-loop transfer function between $R(s)$ and $Y(s)$ is obtained from the block diagram as,

$$G_o(s) = \frac{Y(s)}{R(s)} = \frac{G_c(s)G_p(s)}{1 + G_c(s)G_p(s)} \tag{5}$$

Therefore, the controller $G_c(s)$ will be obtained by rearranging the above equation as follows:

$$\begin{aligned}\frac{G_p(s)}{G_o(s)} &= \frac{1 + G_c(s)G_p(s)}{G_c(s)} \\ &= \frac{1}{G_c(s)} + \frac{G_p(s)G_c(s)}{G_c(s)} = \frac{1}{G_c(s)} + G_p(s)\end{aligned} \tag{6}$$

$$\frac{1}{G_c(s)} = \frac{G_p(s)}{G_o(s)} - G_p(s) = \frac{G_p(s) - G_p(s)G_o(s)}{G_o(s)} \tag{7}$$

$$G_c(s) = \frac{U(s)}{E(s)} = \frac{G_o(s)}{G_p(s)\big(1 - G_o(s)\big)} \tag{8}$$

The desired closed-loop transfer function $G_o(s)$ is considered as follows:

$$G_o(s) = \frac{1}{1 + Ts^\lambda}e^{-sL_p} \tag{9}$$

Thus, FOPPI controller transfer function will be obtained, by substituting Eqs (4) and (9) in (8) as follows:

$$G_c(s) = \frac{1}{\frac{K}{1+Ts^\lambda}e^{-sL_p}}\left(\frac{\frac{1}{1+Ts^\lambda}e^{-sL_p}}{1 - \frac{1}{1+Ts^\lambda}e^{-sL_p}}\right) \tag{10}$$

$$G_c(s) = \frac{1 + Ts^\lambda}{K(1 + Ts^\lambda - e^{-sL_p})} \tag{11}$$

Expressing the controller $G_c(S)$ in terms of input-output relation, the control signal $U(s)$ will be obtained. Thus, the control signal of fractional-order predictive PI (FOPPI) controller is given as follows:

$$\begin{aligned}U(s) = K_p&\left(1 + \frac{1}{T_i s^\lambda}\right)E(s) \\ &- \frac{1}{T_i s^\lambda}(1 - e^{-sL_p})U(s),\ 0 < \lambda < 1\end{aligned} \tag{12}$$

where, $K_p = \frac{1}{K}$, $T_i = T$ and λ is the order of integration. Thus, the designed fractional-order PPI controller in Eq. (12) can be implemented as shown in Fig. 2.

This article has been accepted for publication in a future issue of this journal, but has not been fully edited. Content may change prior to final publication. Citation information: DOI 10.1109/ACCESS.2020.3029068, IEEE Access

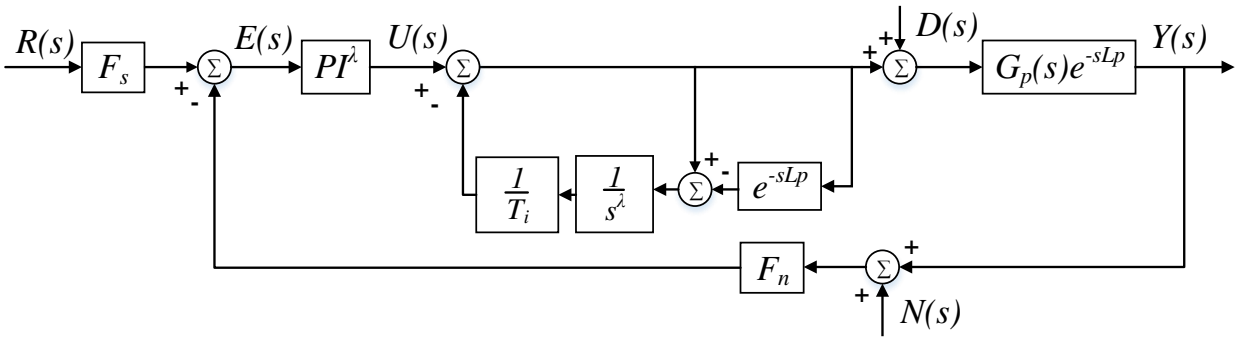

FIGURE 2. **Fractional-order predictive PI controller implementable structure with set-point filter (F_s) and noise filter (F_n).**

C. FILTERING

Placing the different types of filters in the closed-loop control system is illustrated in Fig. 1. Where the F_s and F_n are set-point filter and noise filter for the input signal $R(s)$ and feedback signal $Y(s)$ containing noise. These input signals to the controller are commonly filtered in distinct ways before they are fed into the controller to improve the system performance. Overshoot fluctuations and high-frequency variations in the controller output because of set-point signal $R(s)$ led to the development of a set-point filtering technique. This set-point filter (F_s) separates the varying load disturbance response from the actual set-point response. This will result in a faster process settling because of the reduction in the overshoot and high-frequency issues. On the other hand, noise filter (F_s) is introduced in the feedback signal Y(s) to minimize or nullify the high-frequency noise in the process by compensation technique. Also, by modifying the dynamics of the transfer function this filter improves the controller performance significantly. While designing, it is essential to understand the significance of different types of filters, so they can help in improving the closed-loop feedback performance. Thus, in this research, a simple first-order filter is used for simulation and it is given by:

$$F(s) = \frac{1}{1 + sT_f} \tag{13}$$

where, T_f is the filter time constant.

Various researchers proposed different methods for determining and tuning this filter time constant by using information about the process parameters like peak overshoot, time constant, dead-time, process gain, and peak time. Because of some unnecessary parameters consideration in various designs resulted in extensive calculations made the filter design a complex step. So, in this paper, the conventional and simple method of designing the filter approaches proposed by Hagglund and Normey is used for finding the filter time constant, and later it is compared with the proposed approach. Hagglund approach for calculating the T_f utilizes the integral time of the PI controller (i.e. $T_f = T_i$). This approach may fail to obtain effective performance if the controller is not tuned properly. Also, it did not consider any of the process dynamics which have a huge impact on process settling time overshoot reduction. In Normey approach the process dead-time only used for the filter time constant calculation leaving the process gain (i.e. $T_f = L_n/2$) led to the high overshoot problem.

The above-mentioned method performs well in the lower order process and small dead-time systems with unity process gain (K) and fail to achieve effective performance in higher order and processes with long dead-time. Thus, using the major plant dynamics in the filter time constant will help the filter to perform effectively than the existing methods. In the proposed technique both process gain and dead-time are used for calculating the filter time constant (i.e. $T_f = K/L_n$). The time constants T_{fs} and T_{fn} of the set-point filter and noise filter are added in the process directly since they are considered as non-influencing parameters concerning the controller design.

III. RESULTS AND DISCUSSION

In different applications like industrial electrical drives, precision positioning, unmanned vehicle control, autonomous pathfinders, and trajectory mapping, continuous tracking of the control signal is needed to obtain the optimized path [29], [31], [44]–[46]. In process control applications the main objectives are set-point tracking, disturbance rejection, and noise reduction/regulation [47]–[49]. Thus, the controller signal is shown in all the results and analysis figures to understand more about the effective controller signal amongst all. The simulation results are analyzed and compared in performance conditions like rise time, settling time, overshoot, set-point tracking, disturbance rejection, and noise reduction for different controllers like PI, PPI, FOPI, and FOPPI in the various real-time process models considered. Additionally, set-point and noise filter designs from Hagglund, Normey, and the proposed filter is added with the controller to evaluate their performance for disturbance, overshoot, and noise reduction capabilities. In the feedback loop, a white noise

This article has been accepted for publication in a future issue of this journal, but has not been fully edited. Content may change prior to final publication. Citation information: DOI 10.1109/ACCESS.2020.3029068, IEEE Access

signal of 0.01 magnitude shown in Fig. 3 is injected for examining the noise removal and process signal smoothing characteristics of the filters under comparison.

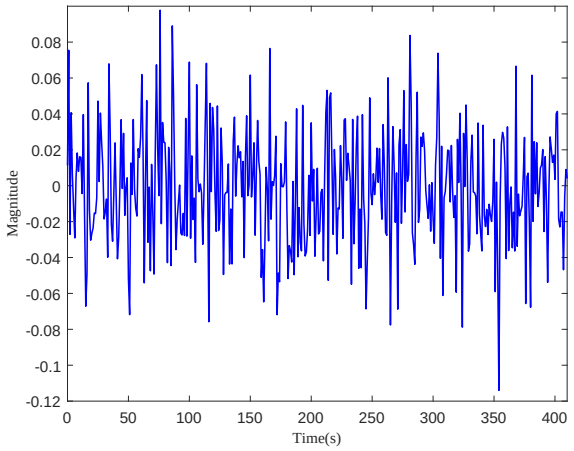

FIGURE 3. Adopted white noise signal profile for simulation.

A. MODEL SELECTION AND CONTROLLER PARAMETERS

In this research real-time process models are used for simulation, which exhibit real industrial plant dynamics and behaviour. For instance, an industrial model of a thermal chamber used by Tan et al. in [11] is utilized as a first-order process model. The other second and third-order process models are given as:

$$G_1(s) = \frac{8e^{-5s}}{1 + 9.13s} \tag{14}$$

$$G_2(s) = \frac{1.3e^{-5s}}{s^2 + 2s + 1} \tag{15}$$

$$G_3(s) = \frac{e^{-10s}}{s^3 + 3s^2 + 3s + 1} \tag{16}$$

Optimised controller parameters for all the controllers obtained are given in Table 2. To get the optimised controller performance, the fractional-order integrator (λ) value is chosen based on trial and error method using the proposed FOPPI controller. The performance under different lambda values is shown in Fig. 4. Additionally, Oustaloup approximation technique parameters used here are frequency range of interest (ω_b,ω_h) = ($10^{-5}, 10^5$) and order of approximation $N = 5$. The parameters are selected based on the works reported in [14], [50]. Thus, transfer of fractional-order integrator is approximated as follows:

$$\frac{1}{s^{0.98}} \approx \frac{\left[s^5 + 9.646 \times 10^4 s^4 + 9.213 \times 10^7 s^3 + 8.798 \times 10^8 s^2 + 8.402 \times 10^7 s + 7.943 \times 10^4\right]}{\left[7.943 \times 10^4 s^5 + 8.402 \times 10^7 s^4 + 8.798 \times 10^8 s^3 + 9.213 \times 10^7 s^2 + 9.646 \times 10^4 s + 1\right]} \tag{17}$$

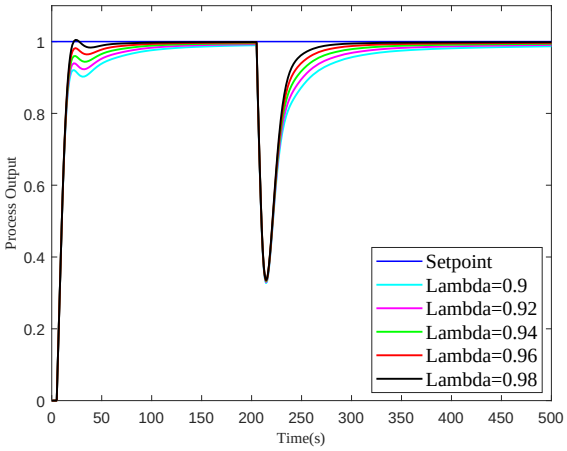

FIGURE 4. Fractional-order integrator (λ) response for different values.

B. FIRST-ORDER SYSTEM

In this subsection, real-time process model of the thermal chamber which is given as $G_1(s)$ in Eq. 14 has been evaluated for set-point tracking, disturbance rejection and variable set-point tracking using the tuned controller parameters in Table 2 and the performance results are shown in Fig. 5. Furthermore, the areas inside the dotted rectangles A,B,C, and D in Fig.5 are enlarged and shown in Fig. 6. Then, the numerical analysis for rise time (t_r), settling time (t_s) and percentage overshoot ($\%OS$) is given in Table 2.

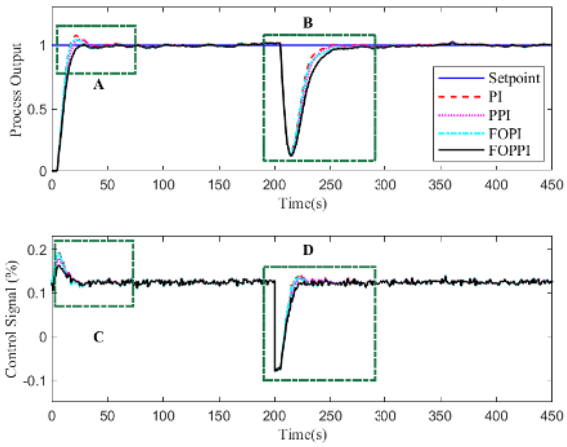

FIGURE 5. Performance comparison of various controllers on the first-order plant for set-point tracking and disturbance rejection.

Observing Fig. 5, 6 and Table 2, it can be easily seen that the proposed fractional-order PPI controller performed better in-terms of set-point tracking and disturbance rejection compared to PI, FOPI and PPI controllers. Though FOPPI is having a slower rise time of 11.8699s, the controller managed to settle faster at 359.4802s while others settled slower at 362.3357s (PI), 361.9219s (FOPI), and 362.1703s (PPI). In peak overshoot, the FOPPI performed well with

This article has been accepted for publication in a future issue of this journal, but has not been fully edited. Content may change prior to final publication. Citation information: DOI 10.1109/ACCESS.2020.3029068, IEEE Access

TABLE 2. Controllers parameters and process models performance in presence of noise.

Plant	Controller	Controller Parameters			Performance		
		K_p	K_i	λ	t_r	t_s	%OS
First-Order	PI	0.1250	0.0137	-	8.4017	362.3357	7.6436
	FOPI	0.1250	0.0137	0.98	8.5636	361.9219	5.1177
	PPI	0.1250	0.0137	-	9.8479	362.1703	4.0463
	FOPPI	0.1250	0.0137	0.98	**11.8699**	**359.4082**	**2.2517**
Second-Order	PI	0.3899	0.1019	-	4.3203	498.4670	16.9419
	FOPI	0.3899	0.1019	0.98	4.3594	498.5718	14.5728
	PPI	0.3899	0.1019	-	6.7458	491.3066	2.0396
	FOPPI	0.3899	0.1019	0.98	**5.6489**	**488.7413**	**2.0660**
Third-Order	PI	0.3301	0.0744	-	8.9926	368.2937	23.0499
	FOPI	0.3301	0.0744	0.98	9.2550	368.1098	17.7708
	PPI	0.3301	0.0744	-	11.5466	367.3590	9.4396
	FOPPI	0.3301	0.0744	0.98	**11.9880**	**354.2014**	**5.4231**

less overshoot of 2.2517% compared to 7.6436, 5.1177, and 4.0463% for PI, FOPI, and PPI respectively. Furthermore, the performance of variable set-point tracking for the plant with all the compared controllers is shown in Fig. 7. The figure clearly shows that the proposed method recovered faster and without overshoot from the effect of the variation in set-point and disturbance compared to other controllers. On the other side, while observing controller action, the aggressiveness of the control signal is more or less the same for all the controllers at the set-point change with less steady stare error.

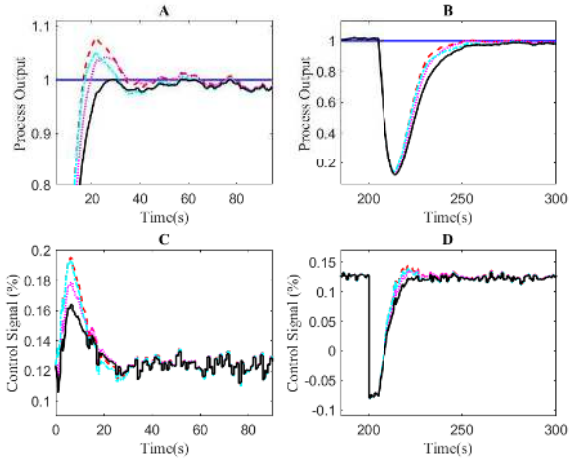

FIGURE 6. Zoomed-in view of Fig. 5 for regions A, B, C and D.

1) Stability Analysis

The graphical representation of the gain margin and phase margins of a control system provides a comprehensive understanding of the system's behavioral dynamics [51], [52]. These control system characteristics are used in the Bode plot, a traditional and most convenient method of finding the stability of the system used by most of the researchers is utilized for this research. Consider the single-input–single-output (SISO) system in the continuous-time domain shown in Fig. 1. Frequency domain representation of First-Order

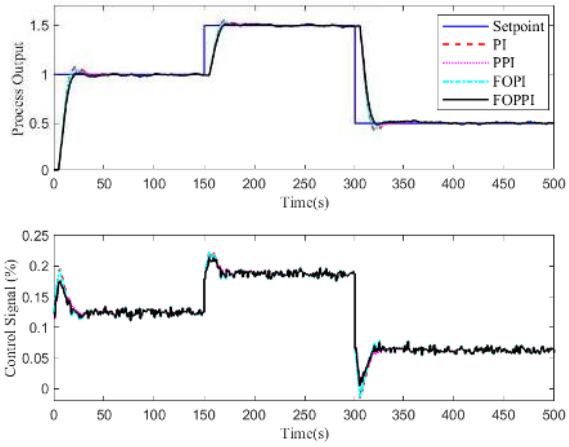

FIGURE 7. Responses of the system with various controllers for variable set-point tracking in the first-order process.

Plus Dead-Time (FOPDT) process will be represented as:

$$G_p(s) = \frac{K}{1+Ts}e^{-sL_p} \implies \frac{K}{1+Tj\omega}e^{-j\omega L_p} \tag{18}$$

The modulus and the argument functions of the above transfer function will be given as,

$$|G_p(j\omega)| = |\frac{K}{1+Tj\omega}| \tag{19}$$

$$\arg(G_p(j\omega)) = \arg(\frac{K}{1+Tj\omega}) - \omega L_p \tag{20}$$

Using the controller parameters from the Table 2 and the process model $(G_1(s))$, the open-loop transfer function of the system will be obtained as given below:

$$G_1(s)G_c(s) = \frac{0.00018769s^{1.96} + 0.0274s^{0.98} + 1}{2.3461e-05s^{1.96} + 0.0017125s^{0.98}}e^{-5s} \tag{21}$$

The above transfer function will be used to obtain the Bode response of the fractional-order predictive PPI controller along with the first order system $(G_1(s))$. Furthermore, this

This article has been accepted for publication in a future issue of this journal, but has not been fully edited. Content may change prior to final publication. Citation information: DOI 10.1109/ACCESS.2020.3029068, IEEE Access

transfer function will be approximated using Oustaloup approximation in the desired frequency range (ω_l, ω_h) to obtain the s^λ. The Oustaloup approximation of s^λ is given as:

$$s^\lambda \approx \omega_h^\lambda \prod_{k=1}^{N} \frac{s+\omega_k'}{s+\omega_k}, \quad 0 < \lambda < 1 \tag{22}$$

where

$$\omega_k' = \omega_l \left(\frac{\omega_h}{\omega_l}\right)^{\frac{2k-1-\lambda}{2N}}$$

$$\omega_k = \omega_l \left(\frac{\omega_h}{\omega_l}\right)^{\frac{2k-1+\lambda}{2N}}$$

The Bode plot analysis of the open loop system with various controller parameters and the corresponding approximated fractional-order transfer function results are shown in Fig. 8. From the Bode plot, based on the gain and phase margin values both the system and the controller are robust and stable in all the considered processes.

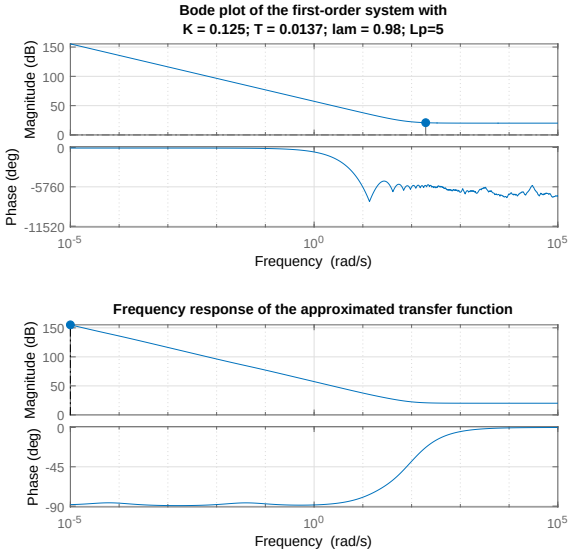

FIGURE 8. Bode plot analysis for the first-order system with controller in presence of time delay.

C. SECOND-ORDER SYSTEM

Performance study of the second-order plant $G_2(s)$ given in Eq. 15 results are given in Table 2. All the analysis and comparisons are performed in a similar fashion to the first-order system. The performance results of this process plant are given in Fig. 9 and the zoomed regions of A, B, C, and D are highlighted in Fig. 10. The figures and numerical analysis represent the analogous trends of the first-order plant is observed in the second-order plant as well. The proposed controller rise time is noticeably increased than the previous first-order process. This resulted in achieving the faster settling time of 488.7413s while others settled at 498.4690, 498.5718, and 491.3066s for PI, FOPI, and PPI respectively. If we observe the Fig. 10 and numerical results in Table 2, during the set-point change most of the controllers had their peak overshoot.

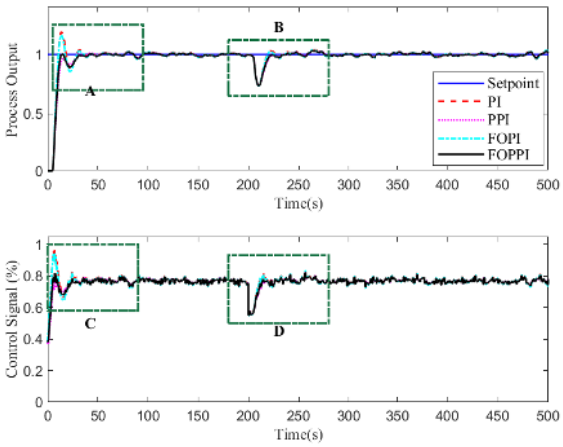

FIGURE 9. Set-point tracking and disturbance rejection performance of various controllers in the second-order process.

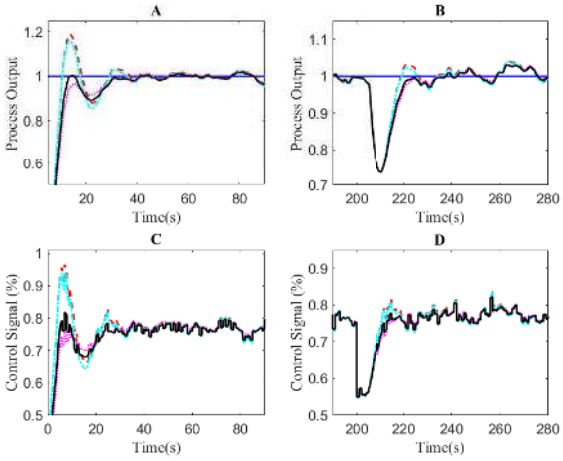

FIGURE 10. Zoomed-in view of Fig. 9 for regions A, B, C and D.

In this plant, the FOPPI controller produced the least overshoot of 2.0660% but it lags behind the PPI by 0.03%. The other controllers PI, FOPI, and PPI have a high peak overshoot of 16.9419, 14.5728, and 2.0396% respectively. In addition, during the variable set-point tracking and disturbance rejection analysis, the FOPPI performed better than all controllers with faster control actions. Since all the compared controllers are from PI family, they continuously manage to give a similar pattern of steady-state error with a close range of each other. Same to the first-order system Bode plot stability analysis, the fractional-order transfer function of the second-order process is given in Eqn. (23) and the respective approximated Bode plot results are illustrated in Fig. 12.

$$G_2(s)G_c(s) = \frac{0.010201s^{1.96} + 0.202s^{0.98} + 1}{0.0039774s^{1.96} + 0.03938s^{0.98}} e^{-5s} \tag{23}$$

This article has been accepted for publication in a future issue of this journal, but has not been fully edited. Content may change prior to final publication. Citation information: DOI 10.1109/ACCESS.2020.3029068, IEEE Access

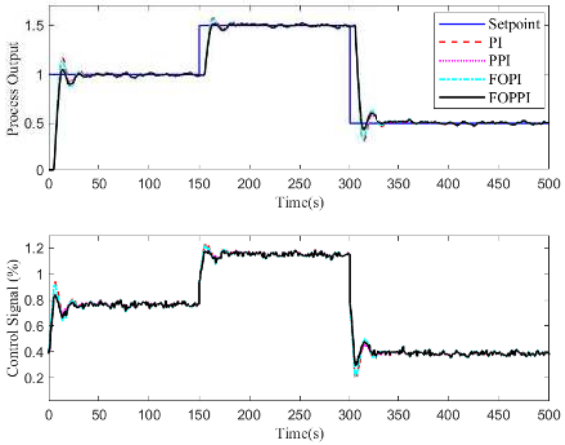

FIGURE 11. **Variable set-point tracking responses of the second-order system with various controllers.**

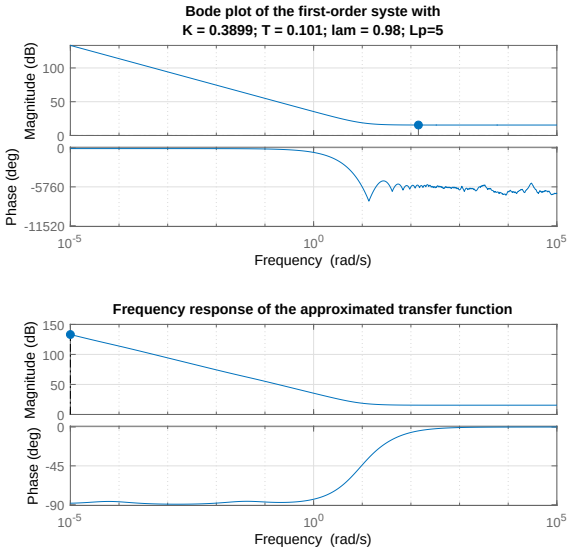

FIGURE 12. **Bode plot analysis for the second-order system.**

D. THIRD-ORDER SYSTEM

The simulation results for the third-order process plant $G_3(s)$ are shown in Fig. 13 and the various regions of interest A, B, C, and D are given in Fig. 14. The numerical analysis of the plant is summarised in Table 2. This plant results also adhere to the trend of the first and second-order process plant performance. The proposed FOPPI has a rise time of 11.9880s which is the slowest one while comparing with PI, FOPI, and PPI of 8.9926, 9.2550, and 11.5466s respectively. However, the FOPPI maintained the faster settling time (354.2014s) including the huge 13.1576 seconds difference in settling time with the second-fastest PPI controller. Also in peak overshoot performance, the FOPPI produced less peak overshoot of 5.4231% comparing the PPI (9.4396%), FOPI (17.7708%), and PI (23.0499%) which is a 17.6268% reduction in overshoot against the highest value. While observing the control signals in Fig. 14, there is aggressive control actions produced by FOPPI and PPI controller to reach the set-point at a faster rate with minimal overshoot. Set-point tracking and disturbance rejection performance of the controllers is shown in Fig. 15. This figure illustrates, all the controllers maintained less steady-state error even during the variation of set-point. In a similar fashion with the first and second-order processes, the fractional-order transfer function of the process is given in Eqn. (24). The Bode plot analysis of this system is shown in Fig. 16.

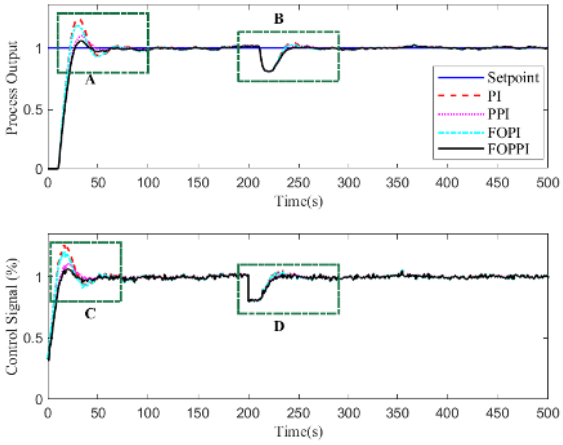

FIGURE 13. **Simulation results of the third order plant with different controllers.**

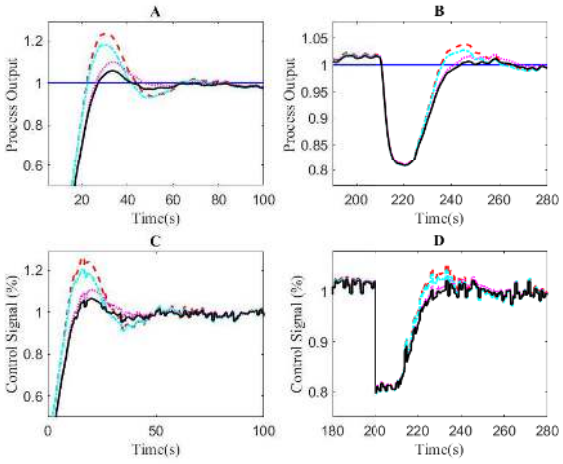

FIGURE 14. **Zoomed-in view of Fig. 13 for regions A, B, C and D.**

$$G_3(s)G_c(s) = \frac{0.0055354s^{1.96} + 0.1488s^{0.98} + 1}{0.0018272s^{1.96} + 0.024559s^{0.98}}e^{-10s} \tag{24}$$

All the performance analysis and comparison results indicate, the FOPPI controller outperformed all the compared controllers in all the process plants. So, the proposed FOPPI

This article has been accepted for publication in a future issue of this journal, but has not been fully edited. Content may change prior to final publication. Citation information: DOI 10.1109/ACCESS.2020.3029068, IEEE Access

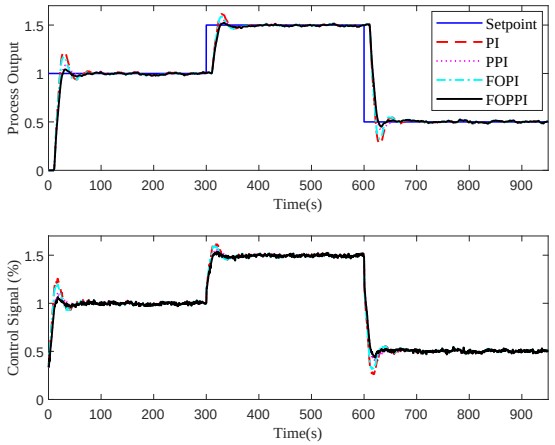

FIGURE 15. Variable set-point tracking responses of the third-order system.

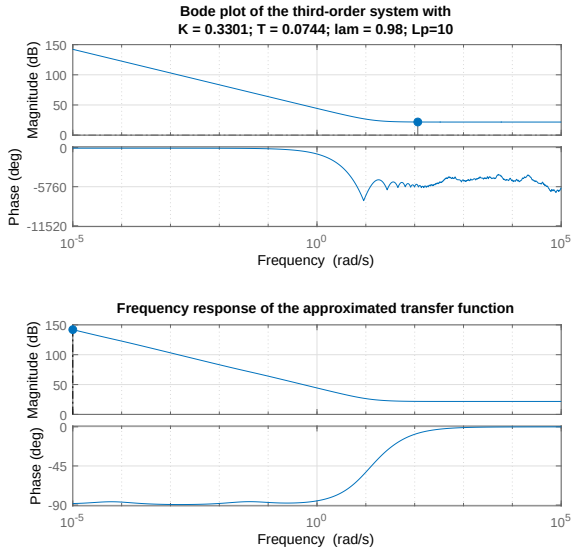

FIGURE 16. Bode plot analysis for the third-order system.

controller alone will be further studied for the performance assessment in the presence of set-point and noise filtering in upcoming simulations.

IV. SET-POINT FILTER

Set-point filters are mostly used along with the PI controller family. As mentioned in the filtering section II-C, this filter is aimed at the reduction of peak overshoot to a desired or tolerable limit. Usually, the selection of this set-point filter depends on various factors and different methods. Mostly this filter is chosen as low-pass in nature with the T_f values of unity or less to ensure the process output and set-point equality in the steady-state period. For the filter evaluation, processes given in the Eqs. 14, 15, and 16 are used with the proposed FOPPI controller. Numerical analysis of the filters and their filter time constant values are given in Table 3.

A. FIRST-ORDER SYSTEM

First-order process plant simulation along with the set-point filtering results are shown in Fig. 17 and the zoomed-in regions of interest A, B, C, and D are given in Fig. 18. Observing the figures and numerical results of this order, there is a huge time difference of 61.0837 seconds in settling time between the process without filter (actual process) (361.4082s) and the proposed filtering (300.3245s), which shows the significant improvements of proposed controller and filtering technique. Remaining Hagglund and Normey filters settled slightly slower than the proposed method of 304.8526 and 301.3071s respectively.

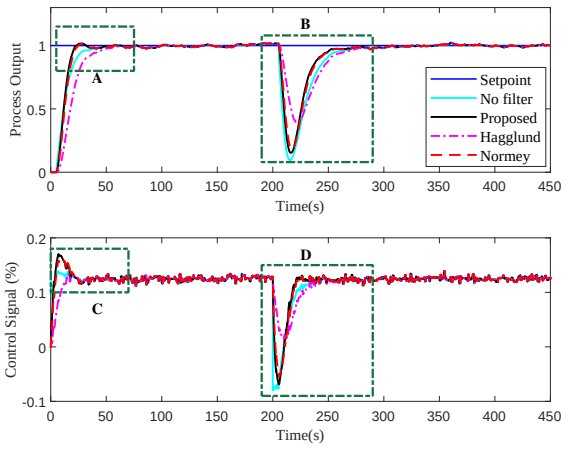

FIGURE 17. First order process plant with various set-point filter.

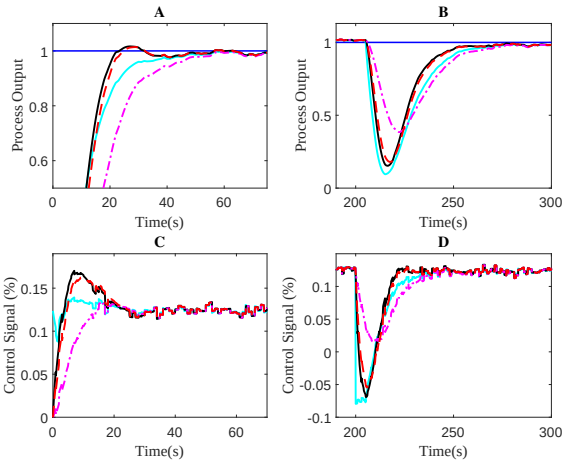

FIGURE 18. Zoomed-in regions of interest A, B, C, and D of Fig.17.

Furthermore, the proposed filtering method achieves the objective of set-point filtering by reducing the peak overshoot of the actual process (2.2517%) with further minimization of 1.8016%. Other filters also reduced little amount with

This article has been accepted for publication in a future issue of this journal, but has not been fully edited. Content may change prior to final publication. Citation information: DOI 10.1109/ACCESS.2020.3029068, IEEE Access

TABLE 3. Various set-point filters performance in different process plants with the FOPPI controller.

Plant	Filter	Filter time constant (T_f)	Performance		
			t_r	t_{s1}	%OS
First-Order	No filter	-	11.8699	359.4082	2.2517
	Proposed filter	1.600	**10.8422**	**300.3245**	**1.8016**
	Hagglund	9.129	22.2326	304.8526	1.9447
	Normey	2.500	11.8971	301.3071	1.9601
Second-Order	No filter	-	5.6489	488.7413	2.0660
	Proposed filter	0.2600	**6.3484**	**423.1467**	**1.7147**
	Hagglund	3.8200	16.6895	427.4958	1.1141
	Normey	2.500	9.6486	426.4957	1.1143
Third-Order	No filter	-	11.9880	354.2014	5.4231
	Proposed filter	0.100	**12.0525**	**295.0385**	**1.6905**
	Hagglund	4.436	15.0968	315.1967	1.8692
	Normey	5.000	15.7516	305.2037	1.7623

the values of 1.9447%, and 1.9601% for Hagglund, and Normey methods. FOPPI performs 1.0277s faster than the actual process in the rise time performance. The Hagglund approach shown faster recovery from the set-point change and disturbance but settled slower than others [See Fig. 18] .

B. SECOND-ORDER SYSTEM

The simulation results of the second-order plant are shown in Fig. 19. The zoomed-in regions of interest A, B, C, and D are given in Fig. 20. The numerical analysis of the above-mentioned figures is given in Table 3. These results indicate the proposed filter and proposed controller combination have the second-fastest rise time of 6.3484s followed by Normey (9.6486s), and Hagglund. (16.6895s) than the actual process (5.6489s).

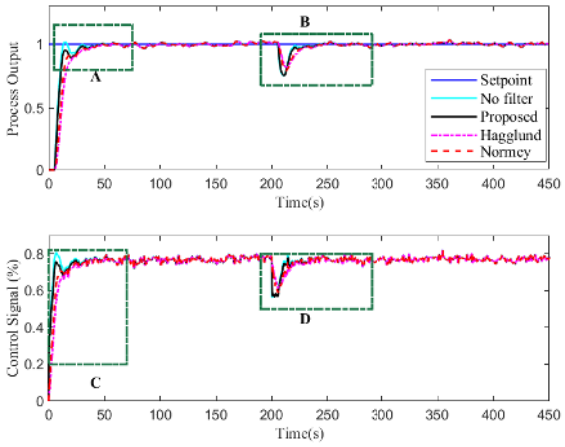

FIGURE 19. Second order process plant with various set-point filter.

In the settling time performance, same combination topped with the fastest settling time of 423.1467s having a 67.4946 seconds time difference from the actual process (490.6413s). Observing Fig. 20 and the numerical analysis, the controller shows aggressive control actions in all the filter combinations which resulted in less peak overshoot for Hagglund (1.1141%) and Normey (1.1143%). The proposed combination had a slightly higher overshoot of 1.7147% than the compared methods but less than the actual process (2.0660%).

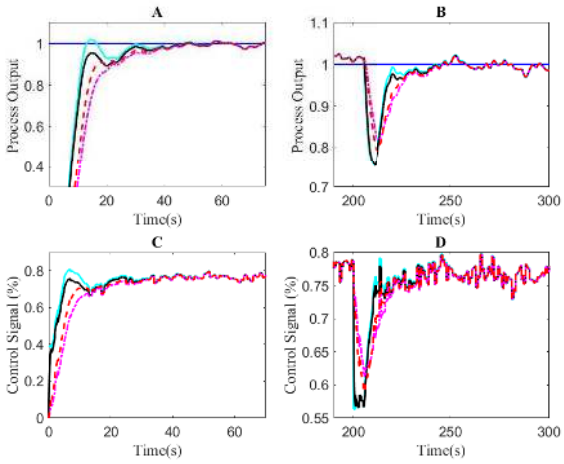

FIGURE 20. Zoomed-in regions of interest A, B, C, and D of Fig.19.

C. THIRD-ORDER SYSTEM

The simulation results of the third-order system are shown in Fig. 21 and the numerical analysis is given in Table 3. The zoomed-in regions of interest A, B, C, and D are shown in Fig. 22. Unlike the first and second-order processes, the third-order performance of the proposed combinations had a rise time of 12.0525s which is marginally slow when compared with the actual process (11.9880s). Likewise, in overshoot analysis, the proposed controller together with all filters combinations performed well. Among those, the proposed filter topped in overshoot reduction with the value of 1.6905% followed by Normey (1.7623%), Hagglund (1.8692%), and actual process (5.4231%). In process settling time, a vast difference of 59.1629 seconds is observed between the actual process (354.2014s) and the proposed approach (295.0385s). While Hagglund and Normey filters settled slightly slower than the proposed method of 315.1967 and 305.2037s respectively. Observing the different control signals in Fig. 22, the proposed approach and the actual process had less aggressive

This article has been accepted for publication in a future issue of this journal, but has not been fully edited. Content may change prior to final publication. Citation information: DOI 10.1109/ACCESS.2020.3029068, IEEE Access

signals than others during the variation in set-point.

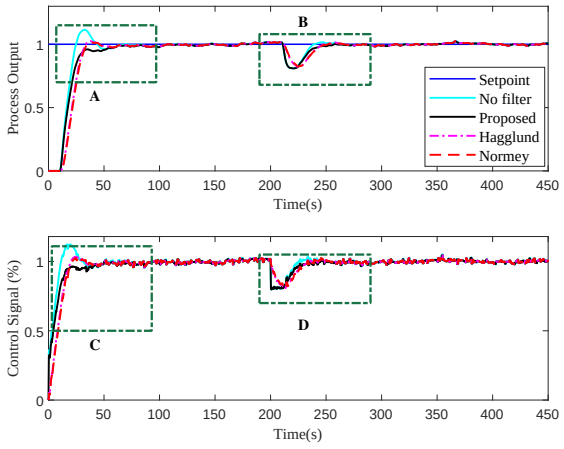

FIGURE 21. Third-order process plant with various set-point filter.

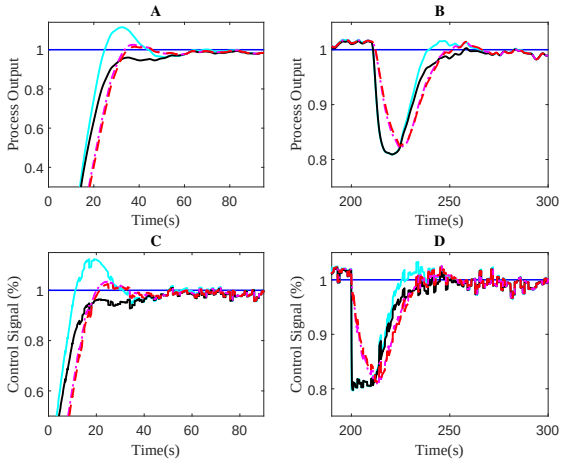

FIGURE 22. Zoomed-in regions of interest A, B, C, and D of Fig.21.

V. NOISE FILTER

When a noisy signal is used in control, filtering the noise component from the feedback signal is essentially needed to avoid the excessive controller output which will result in final control element damages and other loop failures. In this simulation, a first-order filter is used to solve this problem. Due to the absence of derivative actions in the controllers used for simulation, this filter will act as a derivative part to compensate for the noise signal. In the feedback loop a white noise signal of 0.01 magnitude shown in Fig. 3 is injected, for the filter evaluation, processes given in the Eqs. 14, 15, and 16 are used with the proposed FOPPI controller. Numerical analysis of the filters and their filter time constant values are given in Table 4.

A. FIRST-ORDER SYSTEM

Analysis of the noise filter with the FOPPI controller is performed similarly with the previous process plants. Simulation results of the first-order process plant along with the noise filtering are shown in Fig. 23. In contrast with set-point filtering, noise filters produced very high overshoot exceeding the actual process. In that, the Hagglund method produced a twenty-seven times higher overshoot value of 55.8215% than the least one having 2.2517%.

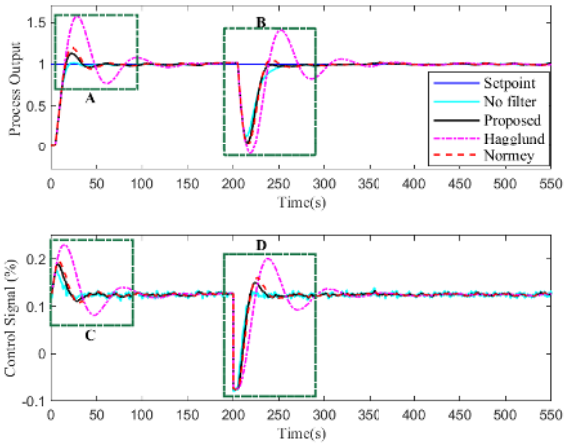

FIGURE 23. First order process plant with various noise filtering.

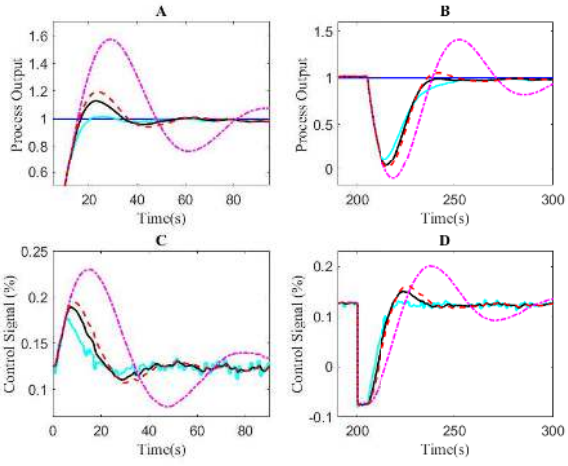

FIGURE 24. Zoomed-in regions of interest A, B, C, and D of Fig.23.

It is noted that, this technique had the overall fastest rise time of 8.1452s but settled very slow at 540.3089s because of the overshoot problem. The proposed and Normey techniques also had a high overshoot of 13.4355 and 20.0537% respectively. Astonishingly, the proposed filter had a faster rise and settling times of 8.7994s and 358.1023s compared to other techniques. However, the proposed filter produced high overshoot compared with the real process. The zoomed-in regions of interest A, B, C, and D are given in Fig. 24.

This article has been accepted for publication in a future issue of this journal, but has not been fully edited. Content may change prior to final publication. Citation information: DOI 10.1109/ACCESS.2020.3029068, IEEE Access

TABLE 4. Various noise filters performance in different process plants with the FOPPI controller.

Plant	Filter	Filter time constant (T_f)	Performance		
			t_r	t_{s1}	%OS
First-Order	No filter	-	11.8699	359.4082	2.2517
	Proposed filter	1.600	**8.7994**	**358.1023**	**13.4355**
	Hagglund	9.129	8.1452	540.3089	55.8215
	Normey	2.500	8.6019	364.4619	20.0537
Second-Order	No filter	-	5.6489	488.7413	2.0660
	Proposed filter	0.2600	**6.0904**	**421.7944**	**3.0542**
	Hagglund	3.8200	6.0243	429.4088	23.6499
	Normey	2.500	6.0402	427.3101	15.4379
Third-Order	No filter	-	11.9880	354.2014	5.4231
	Proposed filter	0.100	**11.3136**	**267.9301**	**5.7872**
	Hagglund	4.436	11.2086	285.0304	27.7576
	Normey	5.000	11.2171	270.3031	30.1781

Paying attention to this figure reveals faster control actions were taken by the proposed filter and controller combo than other filter combinations with the FOPPI controller. After the disturbance injection via set-point change, both proposed and Normey filters had a faster recovery rate because of effective control [See regions B and D of Fig. 24].

B. SECOND-ORDER SYSTEM

The simulation results of the second-order plant are shown in Fig. 25. The zoomed-in regions of interest A, B, C, and D are given in Fig. 26. Table 4 shows only a minor variation in rise time performance is experienced among the compared filtering techniques. In this, the Hagglund technique topped with 6.0243s followed by Normey (6.0402s) and proposed technique (6.0904s). Though there is a small rise time variations, the proposed filter settled faster at 421.7944s with a huge difference of 68.8469 seconds than the actual process (490.6413s). While Hagglund and Normey methods settled at 427.3101 and 426.0506s respectively.

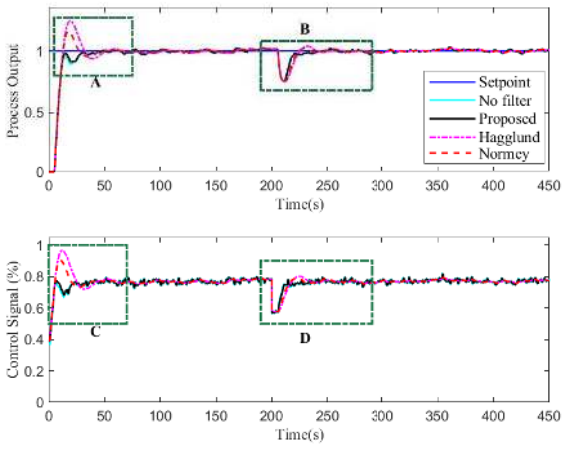

FIGURE 25. Second order process plant with various noise filtering.

Additionally, in overshoot performance, the proposed combinations performed well by having a less peak overshoot of 3.0542% slightly higher than the actual process

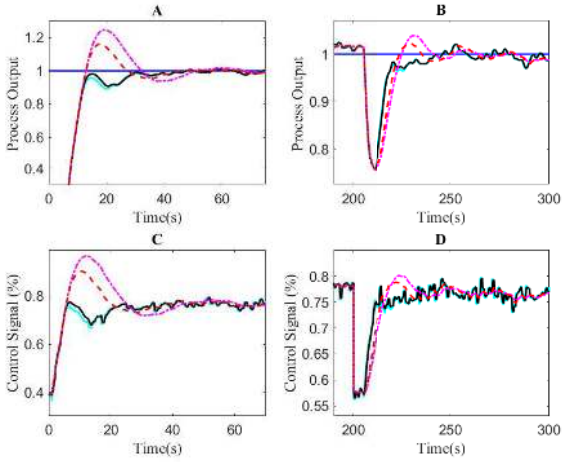

FIGURE 26. Zoomed-in regions of interest A, B, C, and D of Fig.25.

(2.0660%). In a similar fashion with the first-order process, Hagglund and Normey technique produced a high peak overshoot of 23.6499 and 15.4379% which is seven to twelve times higher than the actual process. Variation in set-point severely affects the Hagglund and Normey filter performance, but the proposed filter managed to keep in track with the actual process and settled faster due to aggressive control signal.

C. THIRD-ORDER SYSTEM

The simulation results of the third-order plant are shown in Fig. 27. The zoomed-in regions of interest A, B, C, and D are given in Fig. 28. In this process also, the Hagglund technique had a faster rise with 11.2086s followed by Normey (11.2171s), proposed technique (11.3136s), and actual process (11.9880s). An enormous difference of 86.2713 seconds is observed in the process settling between the proposed filter (267.9301s) and the actual process (354.2014s). In overshoot performance, the proposed filter and the actual process had nearly in-line values of 5.7872% and 5.4231% respectively. In similar to the first and second-order process, Hagglund and Normey technique had a larger peak overshoot of 27.7576%

This article has been accepted for publication in a future issue of this journal, but has not been fully edited. Content may change prior to final publication. Citation information: DOI 10.1109/ACCESS.2020.3029068, IEEE Access

and 30.1781% which are approximately six times higher than the actual process. Observing the various control signals, a more aggressive signal is produced by the proposed filter that resulted in faster recovery during the variation of set-point.

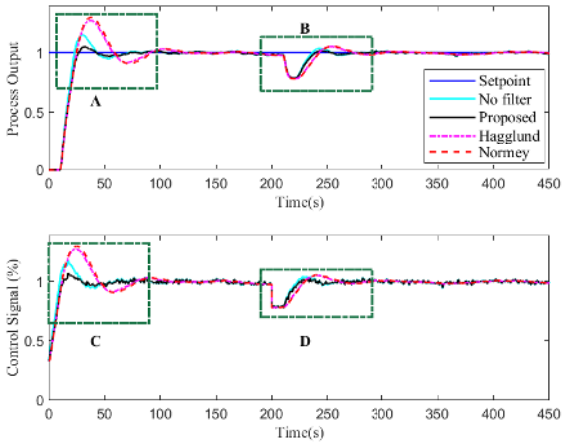

FIGURE 27. Third-order process plant with various noise filtering.

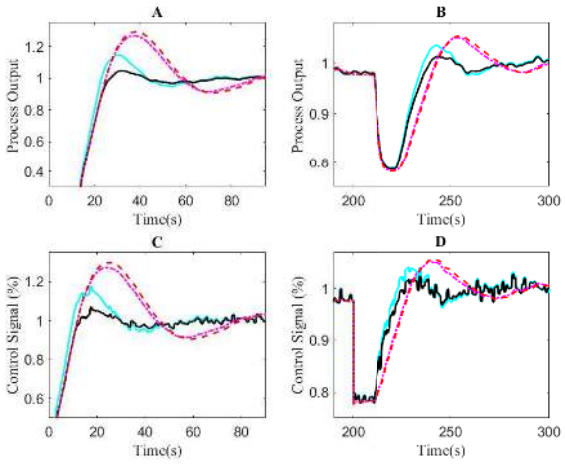

FIGURE 28. Zoomed-in regions of interest A, B, C, and D of Fig.27.

D. REMARKS

The major improvements obtained in process control because of this new controller and filtering are given as follows:

1) Dead-time compensation ability of the Smith predictor based PPI and the fractional-order PI controller's robustness character is retained by the proposed FOPPI controller.
2) Concerning the controller complexity and implementable structure, the proposed controller manages to keep the same number of tuning parameters possessed by conventional PID [See Table 1]. The newly added fractional-order integrator (λ) further enhanced the overall process performance by meeting more frequency-domain requirements.
3) Filters, noise, and disturbance shown in Fig. 2 are made as non-influential constraints while designing the new FOPPI controller, since they don't have any direct relation with the controller design.

E. SUMMARY

Comparative analysis of various controllers namely PI, FOPI, PPI, and FOPPI controllers have allowed us to study their performance in various conditions. Furthermore, filter designs by Hagglund and Normey are compared with the proposed approach to examine their efficiency. Some of the important analyses and findings from the simulation results are highlighted below:

1) In all the process plants considered, the proposed FOPPI controller outperformed the PI, FOPI, and PPI controllers in rise time, settling time, and peak overshoot performances.
2) The proposed controller deals effectively with the variation in set-point and disturbance rejection by taking more aggressive control actions even in process plants with longer dead-time.
3) The proposed set-point filter greatly reduces the overshoot problems in all the process plants.
4) The proposed noise filter results have shown that it immensely smoothens the process signal by making the control signals free from noise.
5) While comparing with the set-point filter, noise filter control signals are smoother which results in reduced offset errors in the process output signal.

VI. CONCLUSION

The design and implementation of a new fractional-order predictive PI (FOPPI) controller for real-time industrial process plants has been presented in this paper. Various performance analyses have been conducted with different controllers to evaluate the proposed controller effectiveness of handling the process with long dead-times and disturbance rejection. Additionally, the set-point and noise filtering technique is introduced in the closed-loop control system. Their simulation results showed effective handling of the overshoot problems, disturbance rejection, set-point tracking, and noise reduction in the process plants considered. In the future, the proposed FOPPI controller will be implemented in the real-time pressure process plant. We will attempt to optimize parameters using any of the most widely used optimization algorithms, since the λ value is chosen based on trial and error method in this research. The real-time implementation will also be carried out in comparison with the wired and wireless process plants to validate the design and latency performance handling by the proposed controller.

REFERENCES

[1] K. J. Åström and T. Hägglund, "The future of pid control," *Control Eng. Practice*, vol. 9, no. 11, pp. 1163–1175, 2001.

[2] K. H. Ang, G. Chong, and Y. Li, "Pid control system analysis, design, and technology," *IEEE Trans. Control Syst. Technol.*, vol. 13, no. 4, pp. 559–576, 2005.

[3] Y. Li, K. H. Ang, and G. C. Chong, "Pid control system analysis and design," *IEEE Control Syst. Mag.*, vol. 26, no. 1, pp. 32–41, 2006.

[4] M. Huba, "Comparing 2dof pi and predictive disturbance observer based filtered pi control," *Journal of Process Control*, vol. 23, no. 10, pp. 1379–1400, 2013.

[5] M. S. Tavazoei, "From traditional to fractional pi control: A key for generalization," *IEEE Ind. Electron. Mag.*, vol. 6, no. 3, pp. 41–51, 2012.

[6] A. Ingimundarson and T. Hägglund, "Performance comparison between pid and dead-time compensating controllers," *J. Process Control*, vol. 12, no. 8, pp. 887–895, 2002.

[7] B. Kristiansson and B. Lennartson, "Evaluation and simple tuning of pid controllers with high-frequency robustness," *J. Process Control*, vol. 16, no. 2, pp. 91–102, 2006.

[8] K. G. Begum, A. S. Rao, and T. Radhakrishnan, "Enhanced imc based pid controller design for non-minimum phase (nmp) integrating processes with time delays," *ISA Trans.*, vol. 68, pp. 223–234, 2017.

[9] M. R. Mataušek and T. B. Šekara, "Pid controller frequency-domain tuning for stable, integrating and unstable processes, including dead-time," *J. Process Control*, vol. 21, no. 1, pp. 17–27, 2011.

[10] Q. H. Seer and J. Nandong, "Stabilising pid tuning for a class of fourth-order integrating nonminimum-phase systems," *Int. J. Control*, vol. 92, no. 6, pp. 1226–1242, 2019.

[11] K.-K. Tan, K.-Z. Tang, Y. Su, T.-H. Lee, and C.-C. Hang, "Deadtime compensation via setpoint variation," *J. Process Control*, vol. 20, no. 7, pp. 848–859, 2010.

[12] S. Srivastava and V. Pandit, "A pi/pid controller for time delay systems with desired closed loop time response and guaranteed gain and phase margins," *J. Process Control*, vol. 37, pp. 70–77, 2016.

[13] K. Bingi, R. Ibrahim, M. N. Karsiti, S. M. Hassan, and V. R. Harindran, "Real-time control of pressure plant using 2dof fractional-order pid controller," *Arab. J. Sci. Eng.*, vol. 44, no. 3, pp. 2091–2102, 2019.

[14] K. Bingi, R. Ibrahim, M. N. Karsiti, and S. M. Hassan, "Fractional order set-point weighted pid controller for ph neutralization process using accelerated pso algorithm," *Arab. J. Sci. Eng.*, vol. 43, no. 6, pp. 2687–2701, 2018.

[15] S. M. Hassan, R. Ibrahim, N. Saad, V. S. Asirvadam, and K. Bingi, "Adopting setpoint weighting strategy for wirelesshart networked control systems characterised by stochastic delay," *IEEE Access*, vol. 5, pp. 25 885–25 896, 2017.

[16] H. Mo and G. Farid, "Nonlinear and adaptive intelligent control techniques for quadrotor uav–a survey," *Asian J. Control*, vol. 21, no. 2, pp. 989–1008, 2019.

[17] J. E. Normey-Rico and E. F. Camacho, "Dead-time compensators: A survey," *Control Eng. Practice*, vol. 16, no. 4, pp. 407–428, 2008.

[18] J. H. Lee, "Model predictive control: Review of the three decades of development," *Int. J. Control Autom. Syst.*, vol. 9, no. 3, p. 415, 2011.

[19] C. D. Tran, R. Ibrahim, V. S. Asirvadam, N. Saad, and H. S. Miya, "Internal model control for industrial wireless plant using wirelesshart hardware-in-the-loop simulator," *ISA Trans.*, vol. 75, pp. 236–246, 2018.

[20] T. Hagglund, "A predictive pi controller for processes with long dead times," *IEEE Control Syst. Mag.*, vol. 12, no. 1, pp. 57–60, 1992.

[21] J. E. Normey-Rico and E. F. Camacho, "Unified approach for robust dead-time compensator design," *J. Process Control*, vol. 19, no. 1, pp. 38–47, 2009.

[22] S. M. Hassan, R. Ibrahim, N. Saad, K. Bingi, and V. S. Asirvadam, "Filtered predictive pi controller for wirelesshart networked systems," in *Hybrid PID Based Predictive Control Strategies for WirelessHART Networked Control Systems*. Springer, 2020, pp. 27–58.

[23] I. Podlubny, "Fractional-order systems and pi/sup/spl lambda//d/sup/spl mu//-controllers," *IEEE Trans. Autom. Control*, vol. 44, no. 1, pp. 208–214, 1999.

[24] C. A. Monje, Y. Chen, B. M. Vinagre, D. Xue, and V. Feliu-Batlle, *Fractional-order systems and controls: fundamentals and applications*. Springer Science & Business Media, 2010.

[25] Y. Chen, I. Petras, and D. Xue, "Fractional order control-a tutorial," in *Proc. Amer. Control Conf., St. Louis, MO, USA*, JUN. 2009, pp. 1397–1411.

[26] A. S. Elwakil, "Fractional-order circuits and systems: An emerging interdisciplinary research area," *IEEE Circuits Syst. Mag.*, vol. 10, no. 4, pp. 40–50, 2010.

[27] P. Shah and S. Agashe, "Review of fractional pid controller," *Mechatronics*, vol. 38, pp. 29–41, 2016.

[28] B. M. Vinagre, C. A. Monje, A. J. Calderón, and J. I. Suárez, "Fractional pid controllers for industry application. a brief introduction," *J. Vib. Control*, vol. 13, no. 9-10, pp. 1419–1429, 2007.

[29] R. Cajo, T. T. Mac, D. Plaza, C. Copot, R. De Keyser, and C. Ionescu, "A survey on fractional order control techniques for unmanned aerial and ground vehicles," *IEEE Access*, vol. 7, pp. 66 864–66 878, 2019.

[30] J. Zhang, Z. Jin, Y. Zhao, Y. Tang, F. Liu, Y. Lu, and P. Liu, "Design and implementation of novel fractional-order controllers for stabilized platforms," *IEEE Access*, vol. 8, pp. 93 133–93 144, 2020.

[31] A. Tepljakov, B. B. Alagoz, C. Yeroglu, E. Gonzalez, S. H. HosseinNia, and E. Petlenkov, "Fopid controllers and their industrial applications: A survey of recent results," *IFAC-PapersOnLine*, vol. 51, no. 4, pp. 25–30, 2018.

[32] X. Zheng and H. Wu, "Design of a robust state estimator for a discrete-time nonlinear fractional-order system with incomplete measurements and stochastic nonlinearities," *IEEE Access*, vol. 8, pp. 10 742–10 753, 2020.

[33] N. Wang, C. Qian, J.-C. Sun, and Y.-C. Liu, "Adaptive robust finite-time trajectory tracking control of fully actuated marine surface vehicles," *IEEE Transactions on Control Systems Technology*, vol. 24, no. 4, pp. 1454–1462, 2015.

[34] M. Li, P. Zhou, Z. Zhao, and J. Zhang, "Two-degree-of-freedom fractional order-pid controllers design for fractional order processes with dead-time," *ISA Trans.*, vol. 61, pp. 147–154, 2016.

[35] T. N. L. Vu and M. Lee, "Smith predictor based fractional-order pi control for time-delay processes," *Korean J. Chem. Eng.*, vol. 31, no. 8, pp. 1321–1329, 2014.

[36] Y. Luo and Y. Chen, "Stabilizing and robust fractional order pi controller synthesis for first order plus time delay systems," *Automatica*, vol. 48, no. 9, pp. 2159–2167, 2012.

[37] I. Birs, C. Muresan, I. Nascu, and C. Ionescu, "A survey of recent advances in fractional order control for time delay systems," *IEEE Access*, vol. 7, pp. 30 951–30 965, 2019.

[38] V. Vijayan and R. C. Panda, "Design of a simple setpoint filter for minimizing overshoot for low order processes," *ISA Trans.*, vol. 51, no. 2, pp. 271–276, 2012.

[39] A. D. Micić and M. R. Mataušek, "Optimization of pid controller with higher-order noise filter," *J. Process Control*, vol. 24, no. 5, pp. 694–700, 2014.

[40] V. Alfaro, R. Vilanova, V. Méndez, and J. Lafuente, "Performance/robustness tradeoff analysis of pi/pid servo and regulatory control systems," in *Proc. IEEE Int. Conf. on Ind. Technol., Vina del Mar, Chile*, 2010, pp. 111–116.

[41] R. Tchamna and M. Lee, "Optimization approach for the analytical design of an industrial pi controller for the optimal regulatory control of first order processes under operational constraints," *J. Taiwan Inst. Chem. Eng.*, vol. 80, pp. 85–99, 2017.

[42] T. Hägglund, "A unified discussion on signal filtering in pid control," *Control Eng. Practice*, vol. 21, no. 8, pp. 994–1006, 2013.

[43] M. Huba, "Filter choice for an effective measurement noise attenuation in pi and pid controllers," in *Proc. IEEE Int. Conf. on Mechatronics (ICM), Nagoya, Japan*, 2015, pp. 46–51.

[44] N. Wang and H. He, "Dynamics-level finite-time fuzzy monocular visual servo of an unmanned surface vehicle," *IEEE Transactions on Industrial Electronics*, 2019.

[45] N. Wang and Z. Deng, "Finite-time fault estimator based fault-tolerance control for a surface vehicle with input saturations," *IEEE transactions on industrial informatics*, vol. 16, no. 2, pp. 1172–1181, 2019.

[46] R. Cui, C. Yang, Y. Li, and S. Sharma, "Adaptive neural network control of auvs with control input nonlinearities using reinforcement learning," *IEEE Transactions on Systems, Man, and Cybernetics: Systems*, vol. 47, no. 6, pp. 1019–1029, 2017.

[47] Z. Gao, "Active disturbance rejection control: a paradigm shift in feedback control system design," in *2006 American control conference*. IEEE, 2006, pp. 7–pp.

[48] J. Han, "From pid to active disturbance rejection control," *IEEE transactions on Industrial Electronics*, vol. 56, no. 3, pp. 900–906, 2009.

[49] L. Sun, Q. Hua, J. Shen, Y. Xue, D. Li, and K. Y. Lee, "Multi-objective optimization for advanced superheater steam temperature control in a 300 mw power plant," *Applied energy*, vol. 208, pp. 592–606, 2017.

[50] A. Tepljakov, "Fomcon: fractional-order modeling and control toolbox," in *Fractional-order Modeling and Control of Dynamic Systems*. Springer, 2017, pp. 107–129.

[51] C.-Y. Kao and B. Lincoln, "Simple stability criteria for systems with time-varying delays," *Automatica*, vol. 40, no. 8, pp. 1429–1434, 2004.
[52] L. H. Keel and S. P. Bhattacharyya, "A bode plot characterization of all stabilizing controllers," *IEEE Transactions on Automatic Control*, vol. 55, no. 11, pp. 2650–2654, 2010.

P.ARUN MOZHI DEVAN (GS'19) received the B.Eng. degree (Hons.) in electronics and instrumentation engineering from the Muthayammal Engineering College, Rasipuram, Tamil Nadu, India, in 2012, and the M.Eng. degree (Hons.) in Control and Instrumentation Engineering from Sri Ramakrishna Engineering College, Coimbatore, Tamil Nadu, India, in 2016. He is currently pursuing the Ph.D. degree with the Electrical and Electronic Engineering Department, Universiti Teknologi Petronas, Perak, Malaysia. He was with Sri Ramakrishna Engineering College as an Assistant Professor (O.G) in the Department of Electronics and Instrumentation Engineering from 2016 to 2018. His current research interests include Fractional-order Control, wireless networked control systems, process control and optimization.

FAWNIZU AZMADI HUSSIN (M'02, SM'14) received the bachelor's degree in electrical engineering from the University of Minnesota, Twin Cities, Minneapolis, MN, USA, in 1999, the M.Eng.Sc. degree in systems and control from the University of New South Wales, Sydney, NSW, Australia, in 2001, and the Ph.D. degree in core-based testing of system-on-a-chip (SoCs) from the Nara Institute of Science and Technology, Ikoma, Japan, in 2008, under the scholarship from the Japanese Government (Monbukagakusho). He is currently an Associate Professor of Electrical & Electronic Engineering at Universiti Teknologi Petronas. He was the Program Manager of Master by coursework program (2009-2013), the Deputy Head of Electrical & Electronic Engineering department (2013-2014) and the Director of Strategic Alliance Office (2014-2018) at UTP. He spent one year as a Visiting Professor at Intel Microelectronics (Malaysia)'s SOC DFx department in 2012-13. He is actively involved with the IEEE Malaysia Section as volunteers since 2009. He was the 2013 & 2014 Chair of the IEEE Circuits and Systems Society Malaysia Chapter and currently serving as the Chair of IEEE Malaysia Section (2019 & 2020)

ROSDIAZLI IBRAHIM (M'09 -SM'16) received the B.Eng. degree (Hons.) in electrical engineering from Universiti Putra Malaysia, Kembangan, Malaysia, in 1996, the M.Sc. degree (Hons.) in automation and control from Newcastle University, Newcastle upon Tyne, U.K., in 2000, and the Ph.D. degree in electrical and electronic engineering from the University of Glasgow, U.K., in 2008. He is currently an Associate Professor with the Department of Electrical and Electronics Engineering, Universiti Teknologi Petronas (UTP), Seri Iskandar, Perak, Malaysia. He is currently the Dean with the Centre of Graduate Studies UTP. His current research interests include intelligent control and non-linear multi-variable process modeling for control application. He is a Registered Engineer with the Board of Engineering Malaysia.

KISHORE BINGI (M'16) received the B.Tech. degree in Electrical and Electronics Engineering from Bapatla Engineering College, Andhra Pradesh, India, in 2012, the M.Tech. degree in Instrumentation and Control Systems from National Institute of Technology (NIT) Calicut, Kerala, India, in 2014, and the Ph.D. degree in the Department of Electrical and Electronic Engineering, Universiti Teknologi PETRONAS (UTP), Perak, Malaysia in 2019. He worked as a Research Scientist and Post-doctoral researcher in the Institute of Autonomous Systems, Universiti Teknologi PETRONAS, Perak, Malaysia from 2019 to 2020. He also worked with TATA Consultancy Service (TCS) as an Assistant Systems Engineer from 2014 to 2015. He is currently an Assistant Professor (Senior Grade) in the Department of Control & Automation, School of Electrical Engineering (SELECT), VIT University, Vellore, India. His current research interests include Non-linear Process Modeling, Fractional-order Control and Optimization.

HAKIM Q. A. ABDULRAB (GS'20) received the B.Eng. (Hons.) degree in electrical and Mechatronics Engineering from Universiti Teknologi Malaysia (UTM), Johor Bahru, Malaysia, in 2013, and the M.Sc.Eng. (Hons.) degree Mechatronics and Automatic Control from Universiti Teknologi Malaysia (UTM), Johor Bahru, Malaysia, in 2019. He is currently pursuing the Ph.D. degree with the Electrical and Electronic Engineering Department, Universiti Teknologi Petronas (UTP), Perak, Malaysia. He worked as a teaching engineer in faculty of engineering and IT, Taiz University, Yemen from 2013 to 2016. His current research interests include wireless networked control systems, and fault tolerant control.